

Challenging of AS160/TBC1D4 Alters Intracellular Lipid milieu in L6 Myotubes Incubated With Palmitate

AGNIESZKA MIKŁOSZ,¹ BARTŁOMIEJ ŁUKASZUK,^{1*}
MAŁGORZATA ŻENDZIAN-PIOTROWSKA,² JUSTYNA BRAŃSKA-JANUSZEWSKA,³
HALINA OSTROWSKA,³ AND ADRIAN CHABOWSKI¹

¹Department of Physiology, Medical University of Białystok, Białystok, Poland

²Department of Hygiene, Epidemiology and Ergonomics, Medical University of Białystok, Białystok, Poland

³Department of Biology, Medical University of Białystok, Białystok, Poland

The Akt substrate of 160 kDa (AS160) is a key regulator of GLUT4 translocation from intracellular depots to the plasma membrane in myocytes. Likely, AS160 also controls LCFAs transport, which requires relocation of fatty acid transporters. The aim of the present study was to determine the impact of AS160 knockdown on lipid milieu in L6 myotubes incubated with palmitate (PA). Therefore, we compared two different settings, namely: 1) AS160 knockdown prior to palmitate incubation (pre-PA-silencing, AS160⁻/PA); 2) palmitate incubation with subsequent AS160 knockdown (post-PA-silencing, PA/AS160⁻). The efficiency of AS160 silencing was checked at mRNA and protein levels. The expression and localization of FA transporters were determined using Western Blot and immunofluorescence analyses. Intracellular lipid content (FFA, DAG, TAG, and PL) and FA composition were estimated by GLC, whereas basal palmitate uptake was analyzed by means of scintigraphy. Both groups with silenced AS160 were characterized by a greater expression of FA transporters (FAT/CD36, FATP-1, 4) which had contributed to an increased FA cellular influx. Accordingly, we observed that post-PA-silencing of AS160 resulted in a marked decrement in DAG, TAG, and PL contents, but increased FFA content (PA/AS160⁻ vs. PA). The opposite effect was observed in the group with pre-PA-silencing of AS160 in which AS160 knockdown did not affect the lipid pools (AS160⁻/PA vs. PA). Our results indicate that post-PA-silencing of AS160 has a capacity to decrease the lipotoxic effect(s) of PA by decreasing the content of lipids (DAG and PL) that promote insulin resistance in myotubes.

J. Cell. Physiol. 232: 2373–2386, 2017. © 2016 The Authors. *Journal of Cellular Physiology* Published by Wiley Periodicals Inc.

Insulin resistance is an early defect occurring in the pathogenesis of type 2 diabetes mellitus (T2DM). Nowadays, changes in our lifestyle such as increased intake of high-caloric food combined with physical inactivity greatly contributed to the dramatic increase in the worldwide incidence of T2DM (Manrique and Sowers, 2014). The prevalence of T2DM continues to grow affecting 415 million adults worldwide in 2015 (Cho et al., 2015). Many studies have indicated that dysregulation of fatty acid metabolism in skeletal muscle is the main culprit responsible for the development insulin resistance and T2DM (Samuel et al., 2010; Eckardt et al., 2011; Martins et al., 2012). In obese/type-2-diabetic individuals lipolysis is commonly elevated, thus, leading to an increased concentration of circulating free fatty acids (FFA) and subsequent intramyocellular lipid (IMCL) accumulation (Blaak, 2005). IMCL represent a significant substrate source for biosynthesis of other lipids, namely diacylglycerol (DAG) and ceramide (CER) that may interfere with insulin signaling pathway (Mukherjee et al., 2013). Recent years investigation have proven that long chain fatty acids (LCFAs) require protein transporters, such as fatty acid translocase (FAT/CD36), fatty acid transport proteins (FATPs), and plasma membrane fatty acid-binding protein (FABPpm) in order to cross the membrane barrier of a cell (Schwenk et al., 2010). It was observed that the CD36 mRNA and its protein level were significantly increased in both rodent and human skeletal muscles in response to several days of high-fat diet feeding (Cameron-Smith et al., 2003). Additionally, the defective uptake and utilization of LCFAs in skeletal muscle, heart, and adipocytes were observed in CD36 knockout mice (Coburn et al., 2000). Moreover, constantly increased fatty acids transport rates have been connected with permanent relocation of FAT/CD36 to the plasma membrane in T2DM and diet induced insulin resistance (Ouwens et al., 2007).

Skeletal muscle accounts for the majority (70–90%) of insulin-mediated glucose tissue-storage (in postprandial conditions) and for that reason the defects of insulin action in this tissue are central to the pathogenesis of T2DM (Choi and Kim, 2010; Cartee, 2015a). Insulin stimulation leads to rapid and reversible redistribution of glucose transport proteins (GLUT-4) from intracellular vesicles to the plasma membrane (Chadt et al., 2015). The Akt substrate of 160 kDa, also known as AS160 (TBC1D4), is a key protein that through its

This is an open access article under the terms of the Creative Commons Attribution-NonCommercial-NoDerivs License, which permits use and distribution in any medium, provided the original work is properly cited, the use is non-commercial and no modifications or adaptations are made.

Conflicts of interest: The authors declare no conflict of interests.

Contract grant sponsor: National Science Centre (NSC), Medical University of Białystok;

Contract grant numbers: 2012/07/N/NZ3/01615, 133-18768L, 154-18702, 104/KNOW/15.

*Correspondence to: Bartłomiej Łukaszuk, Department of Physiology, Medical University of Białystok, Mickiewiczza 2C street, 15-222 Białystok, Poland. E-mail: bartlomiej.lukaszuk@umb.edu.pl

Manuscript Received: 12 May 2016

Manuscript Accepted: 5 October 2016

Accepted manuscript online in Wiley Online Library (wileyonlinelibrary.com): 7 October 2016.

DOI: 10.1002/jcp.25632

interactions with Rab proteins regulates the translocation of GLUT4 (Frosgig and Richter, 2009; Cartee, 2015b; Hargett et al., 2015). However, to the best of our knowledge little is known about the potential involvement of ASI60 in facilitated fatty acids uptake in muscle. So far, only one study conducted in cardiomyocytes indicated that trafficking of CD36, a most important facilitator of FA uptake, is regulated by ASI60 in a similar way to that of GLUT4 (Samovski et al., 2012). Apart from that study, also our previous work documented the importance of ASI60 modulation with respect to fatty acids transporters expression and lipid profile in L6 myotubes (Miklosz et al., 2016). We demonstrated that moderate inactivation of ASI60 resulted in greater expression of fatty acids transporters, namely FABPpm and FAT/CD36, together with a slightly increased FAs cellular influx (Miklosz et al., 2016). However, molecular regulation of fatty acids uptake by ASI60 and its potential contribution to the etiology of insulin resistance in skeletal muscle still remains elusive. The aim of this study was to determine the impact of ASI60 silencing on intramyocellular lipid milieu and FA transporters expression in L6 myotubes incubated with palmitate. In this study, we attempted to examine whether silencing of ASI60 favors subsequent intracellular influx of palmitate, due to the lower transport of glucose, and in addition whether palmitate stimulation alters ASI60 action in L6 myotubes. Therefore, in an effort to better understand the role of ASI60 in the fatty acid induced insulin resistance the present study compares two different settings, namely: 1) ASI60 knockdown prior to palmitate incubation (pre-PA-silencing of ASI60, ASI60⁻/PA), and 2) palmitate incubation with subsequent ASI60 knockdown (post-PA-silencing of ASI60, PA/ASI60⁻).

Materials and Methods

Cell cultures

All experiments were performed on rat-derived L6 skeletal muscle cells purchased from the ATCC (American Type Culture Collection) and in accordance with the manufacturer's recommendations (Seyoum et al., 2011). Briefly, L6 cells were cultured in high-glucose (4.5 g/L) Dulbecco's modified Eagle's medium (DMEM) containing 10% FBS (Fetal Bovine Serum) and 1% antibiotic/antimycotic in a 5% CO₂ humidified atmosphere at 37°C. The cells were cultivated up to the ~80% confluence. At that time point medium was changed to DMEM containing 2% HS (horse serum) for the induction of differentiation into myotubes. The differentiation medium was replaced every 48–72 h. The cells were ready for further experiments when visual inspection confirmed that cells were differentiated (usually about 7 days, when more than 90% of the cells were fused into myotubes).

RNA interference (RNAi)—gene silencing

ASI60 was successfully knocked down using gene silencing method and according to the manufacturer's recommendations (Thermo Fisher Scientific, former Lifetechnologies, former Invitrogen, Waltham, MA) (Constantinescu and Turcotte, 2013). The day before transfection, the cells were transferred to a growth medium without antibiotics. L6 myotubes grown in 6-well culture plates were transfected with 100 nM siRNA (for ASI60) or negative-control (noncoding/non-targeting siRNA) with Opti-MEM[®] I Reduced Serum Medium in DMEM without antibiotics. Lipofectamine mixture was removed after 6 h of incubation. Afterwards, the cells were incubated at 37°C in a 5% CO₂ atmosphere for 48 h until the evaluation (RT-PCR) of the gene knockdown was performed. Three commercially available small interfering RNA (siRNA) oligonucleotide sequences for ASI60 were purchased (GAGUCG CAG AUGGCCACGUUU; GCACAAAGAGAA AGCUGAAUUUGCA; CCAGAGCCUGGACUUAAGCCAGUAU A), while for further experiments we chose the one with the highest desired efficiency (the underlined one).

Fatty acid treatment

Palmitate was administered to the cells after conjugation with fatty acid-free bovine serum albumin (BSA, Sigma–Aldrich, St. Louis, MO). Briefly, palmitate stock solution was prepared by dissolving palmitate into a solution containing absolute ethanol and 1 M NaOH, heating to 70°C and conjugating with 10% of BSA. Then, stock solution was diluted in serum free-DMEM and L6 myotubes were incubated with palmitic acid at the concentration of 0.75 mM for 16 h. At the end of each experimental set the cells were microscopically examined for morphology and viability (i.e., Trypan blue staining). In one of the groups, ASI60 was knocked down (for 48 h) using gene silencing method before incubation with palmitate (0.75 mM) for the next 16 h (designation of the group: pre-PA-silencing of ASI60, ASI60⁻/PA). In the second set of experiment, the cells were incubated with palmitate (0.75 mM) for 16 h and then subjected to knockdown of ASI60 (designation of the group: post-PA-silencing of ASI60, PA/ASI60⁻).

Real-time PCR

ASI60 mRNA level was measured with the use of real-time quantitative PCR. The RNA was extracted from L6 cultured myotubes using the RNeasy Mini Kit (Qiagen, Venlo, Netherlands) in accordance with the manufacturer's instructions. Following RNA purification, DNase treatment (Ambion[®], Thermo Fisher Scientific, Waltham, MA) was performed to ensure that there was no contamination of genomic DNA. The quality of RNA was verified by measuring the samples absorbencies at 260 and 280 nm and assessed by running the agarose electrophoresis with ethidium bromide. The RNA was reversely transcribed into cDNA using iScript cDNA Synthesis Kit (Bio-Rad, Hercules, CA), while primers were designed using Beacon Designer Software (Premier Biosoft, Palo Alto, CA). Real-time PCR was performed using SYBR Green JumpStart Taq ReadyMix (Sigma–Aldrich) via a Bio-Rad Chromo4 system. PCR efficiency was examined by serially diluting template cDNA, and a melt curve was performed at the end of each reaction to verify PCR product specificity. A sample containing no cDNA was used as a negative control to verify the absence of primer dimers. The results were normalized to cyclophilin A expression measured in each sample. For further studies sequence with the highest desired efficiency was chosen (as underlined). Primer sequences for ASI60: 1) F: 5'-AGA AGG GGT CCC TAA AAG TCG GC-3'; R: 5'-GTT GGG CAA TCT GTG TCT CAG GC-3'; 2) F: 5'-AGA TTG CCC AAC AAA CAC CAG CC-3'; R: 5'-TGA GTG GGA AAA GTC CTC CCC AA-3'; 3) F: 5'-CTC TGG AGA AGC TGG AGA GAG CG-3'; R: 5'-GGC CTG AAT TTT AGC GTT AGC CA-3'. Cyclophilin A: 1) F: 5'-TGT CTC TTT TCG CCG CTG GCT G-3'; R: 5'-CAC CAC CCT GGC ACA TGA ATC C-3'; 2) F: 5'-GTC AAC CCC ACC GTG TTC TTC G-3'; R: 5'-TGT GAA GTC ACC ACC CTG GCA C-3'; 3) F: 5'-AGCACT GGG GAG AAA GGA TT-3'; R: 5'-AGA TGC CAG GAC CTG TAT GC-3'.

Immunofluorescence staining

L6 cells grown on cover-slips were washed with PBS and then fixed in 4% paraformaldehyde in PBS for 10 min and blocked in 5% normal donkey serum (Sigma–Aldrich) at room temperature for 60 min. Next, the cells were incubated with: goat polyclonal anti-TBC1D4 antibody (1:100, Santa Cruz Biotechnology, Dallas, TX), goat polyclonal anti-FATP4 antibody (1:100, Santa Cruz Biotechnology), rabbit polyclonal anti-FATP1 antibody (1:100, Santa Cruz Biotechnology), rabbit polyclonal anti-CD36 antibody (1:100, Novus Biologicals, CO) and rabbit polyclonal anti-FABPpm antibody (1:100, Abcam, Cambridge, UK) for 60 min at RT. After incubation, the cells were washed three times with PBS and incubated in donkey anti-goat IgG conjugated with Alexa543 (1:200, Molecular Probes) or donkey anti-rabbit IgG conjugated with Alexa488 (1:200, Molecular Probes) at RT for 1 h. Then, the cells were washed three

times in PBS and stained with 4',6'-diamidino-2-phenylindole (DAPI, Sigma–Aldrich) for 10 min to indicate the nucleus. The samples were washed twice with PBS and mounted with fluorescent medium (Medium Coverquick, Hygeco), dried overnight and stored in the dark until assessment. Immunolabeled cells were analyzed using Nikon Digital Sight DS-Fi1 camera and a fluorescence microscope (Nikon ECLIPSE Ti/CI Plus, equipped with three filters DAPI [blue], FITC [green], and TRITC [red] [excitation wavelength/emission filter: 405/450 nm, 488/515 nm, 543/605 nm, respectively]). No fluorescence signal was detected when L6 muscle cells were incubated with secondary antibodies alone (data not shown). The protein intensity staining was measured using ImageJ software. At least 6 pictures of different areas of each treatment group were taken, independently analyzed and one representative image for each study group was presented.

Protein extraction and Western Blot

For the detection of protein content Western blotting procedures were applied as described previously (Chabowski et al., 2013; Lukaszuk et al., 2015; Miklosz et al., 2016). Briefly, the cells were lysed in ice-cold RIPA (radioimmunoprecipitation assay) buffer with protease and phosphatase inhibitors and sonicated for 1 min at 4°C. Bicinchonnic acid method with BSA serving as a protein standard was used for protein concentration assessment. Samples (60 µg of the total protein) were resolved using 10% SDS-PAGE and wet-transferred to nitrocellulose membranes (0.75 A for 1 h). Membranes were then blocked for 90 min at room temperature in 5% nonfat dry milk in TBST. Then membranes were immunoblotted with primary antibodies purchased from Santa Cruz Biotechnology (ASI60, FAT/CD36, FABPpm, FATP-1, 4) and Novus Biologicals (β-actin). Membranes were then incubated with anti-rabbit or anti-goat IgG horseradish peroxidase-conjugated secondary antibody (Santa Cruz Biotechnology). The bands were visualized using an enhanced chemiluminescence substrate (Thermo Fisher Scientific, Waltham, MA) and quantified densitometrically (Biorad). Ponceau staining technique was performed to confirm equal protein loading on the blot membrane. The protein expression (Optical Density Arbitrary Units) was normalized to β-actin expression. Control group was set at 100 and the experimental groups were expressed in relation to the control.

[9, 10-3H (N)]—palmitic acid uptake

Palmitic acid uptake was performed according to the Chavez and Summers protocol (Chavez and Summers, 2003). Briefly, L6 myotubes were incubated with incubation medium supplemented with palmitic acid (Sigma–Aldrich) bound to fatty acid-free bovine serum albumin (Sigma–Aldrich, St. Louis, MO) with addition of radiolabelled [9,10-3H] palmitic acid (Perkin Elmer) at the specific activity of 1 µCi mL⁻¹. After 5 min ice-cold PBS was added to terminate palmitate uptake and the cells were immediately solubilized in 0.05 N NaOH. Subsequently, the resulting fluid was placed in 5 ml vials and taken for liquid scintillation counting (Beckman, Brea, CA). Radioactivity was normalized with respect to protein concentration.

Lipid analyses

The lipids (TAG, DAG, PL, and FFA) were extracted from L6 myotubes using Folch method (Folch et al., 1957) modified according to van der Vusse (van der Vusse et al., 1980). The cells were extracted using chloroform-methanol (2:1, vol/vol) solution containing butylated hydroxytoluene (0.01%) as an antioxidant and heptadecanoic acid as an internal standard. After extraction, the lipid samples were separated by thin-layer chromatography (TLC) silica plates (Kieselgel 60, 0.22 mm, Merck, Darmstadt, Germany) with a heptane: isopropyl ether: acetic acid (60:40:3, vol/vol/vol) resolving solution. Then fatty acids, together with methylpentadecanoic acid (Sigma–Aldrich) used as an internal standard, were transmethylated in

14% methanolic solution of boron trifluoride. Individual fatty acid methyl esters (FAMES) were identified and quantified according to the retention times of standards by gas liquid chromatography (Hewlett-Packard 5890 Series II gas chromatograph with Varian CP-SIL capillary column). Total content of FFA, DAG, TAG, and PL was estimated as the sum of the particular FA species in the assessed fraction and expressed in nanomoles per milligram of protein. We have also presented fatty acid profile of each lipid fractions examined, that is, saturated and mono- and polyunsaturated fatty acids.

Statistical analysis

The analyses were conducted using R statistical software (version 3.1.2). Analysis of variance (ANOVA) followed by pairwise Student's *t*-test (with the Holm *P*-value multiplicity correction) was applied to test the existence of differences between the studied groups. Whenever their assumptions did not hold the Kruskal–Wallis rank test with the subsequent pairwise Wilcoxon test (with the Holm *P*-value multiplicity correction) were conducted. Any differences with adjusted *P*-values <0.05 were considered to be statistically significant. The displayed data are expressed as the mean ± standard deviation. As stated in the Materials and Methods section in order to avoid any unspecific effects of our technique (siRNA silencing with Lipofectamine reagent) we have employed negative control (NC, NC/PA) groups (containing non-targeting siRNA fragment). Therefore, the results for the ASI60 knockdown groups were compared with the abovementioned groups. For clarity only pre- and post-PA-silencing of ASI60 groups (ASI60⁻/PA and PA/ASI60, respectively) and the appropriate control groups (NC, NC/PA) are presented.

Results

First, we assessed the effectiveness of ASI60 knockdown. As previously reported by us (Miklosz et al., 2016) ASI60 silencing measured 48 h after the procedure, resulted in 82% decrease in its mRNA and 25% decrease in its protein content, as confirmed by RT-PCR and Western Blot, respectively (ASI60⁻ vs. Ctrl, *P* < 0.05). Additionally, in order to evaluate whether TBCID1 (ASI60 paralog) could compensate for the lack of ASI60 in the silenced myotubes (ASI60⁻) we determined TBCID1 expression. As illustrated in Figure 1B, there were no significant differences in the expression of TBCID1 between the studied groups (*P* > 0.05, Fig. 1B).

Effects of pre- and post-PA-silencing of ASI60 on the ASI60 immunofluorescence intensity in L6 myotubes

Immunofluorescence microscopy had shown that palmitate stimulation itself significantly increased ASI60 immunofluorescence intensity (+30%, *P* < 0.05, Fig. 1A). However, neither pre- nor post-PA-silencing of ASI60 had any additional effect on the ASI60 intensity of staining as compared to the ASI60 silenced group alone (ASI60/PA⁻ and PA/ASI60⁻ vs. ASI60⁻, +5%, +32%, *P* > 0.05, Fig. 1A). The omission of ASI60 primary antibody step resulted in no staining, thus confirming the secondary antibody specificity and the absence of cellular autofluorescence (negative control, data not shown).

Effects of pre- and post-PA-silencing of ASI60 on the expression and localization of fatty acid transporters (FAT/CD36, FABPpm, FATP-1, 4) in L6 myotubes

Interestingly, palmitate treatment did not significantly change total expression of fatty acid transporters (i.e., FAT/CD36, FABPpm, and FATP-1) and only a trend toward the reduction of FATP-4 content was noticed (PA vs. Ctrl, *P* > 0.05, Fig. 2A). However, the pre- and post-silencing of ASI60 combined with palmitate treatment

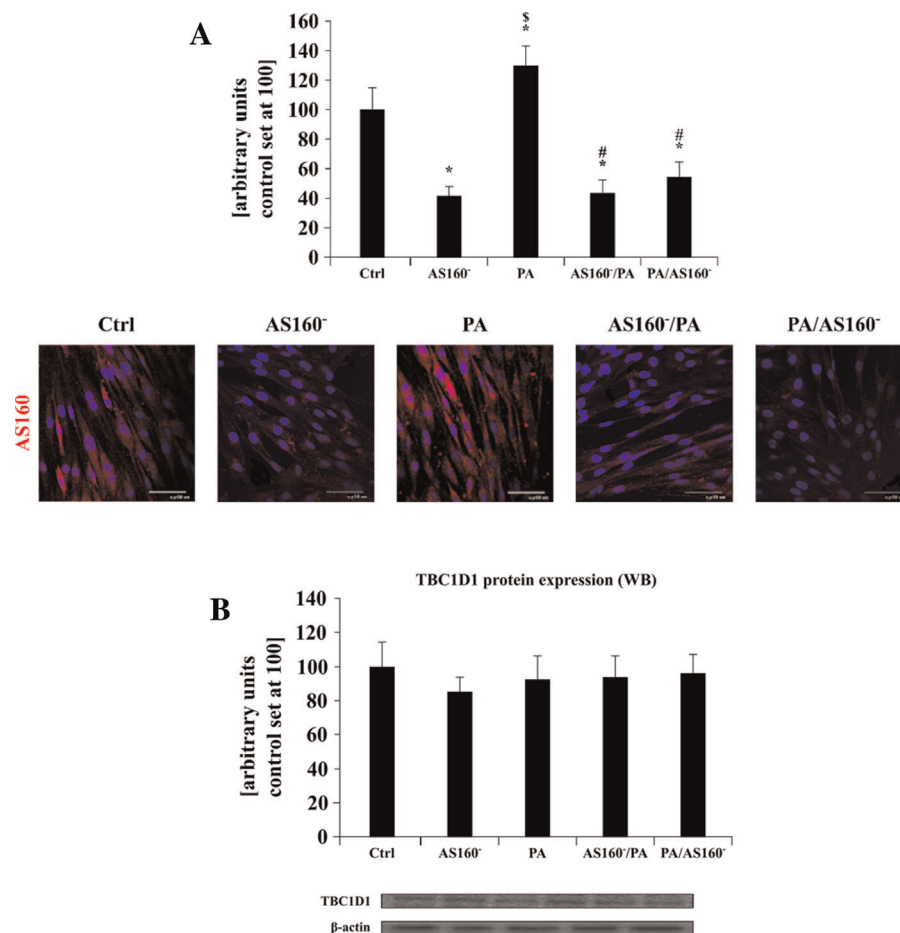


Fig. 1. The effect of pre- and post-PA-silencing of ASI60 on the ASI60 staining intensity and its intracellular localization (A) and the expression of TBC1D1 (B) (analyzed by the means of confocal microscopy [A] and Western Blot [B]) in L6 myotubes. Data are based on 6 independent determinations for each treatment (bar height = mean, whiskers = SD). Values are expressed in arbitrary units; control group was set as 100. Representative immunofluorescent images are shown. ANOVA followed by pairwise Student's *t*-test (with the Holm *P*-value multiplicity correction) was applied. Whenever their assumptions did not hold the Kruskal–Wallis rank test with the subsequent pairwise Wilcoxon test (with the Holm *P*-value multiplicity correction) was conducted. **P* < 0.05 significant difference: control (CTRL) versus treatment, #*P* < 0.05 significant difference: palmitate (PA) versus treatment, §*P* < 0.05 significant difference: knockdown of ASI60 (ASI60⁻) versus treatment.

resulted in an increase in the expression of the aforementioned transporters (ASI60/PA⁻ and PA/ASI60⁻ vs. PA; FAT/CD36: +67%, +72%, FATP-1: +44%, +59%, and FATP-4: +64%, +59%, respectively, *P* < 0.05, Fig. 2A). On the other hand, the expression of FABPm was decreased in both settings with ASI60 silencing as compared to the palmitate treated myotubes (ASI60⁻/PA and PA/ASI60⁻ vs. PA; -30% and -28%, respectively, *P* < 0.05, Fig. 2A). These results were similar to the observed immunofluorescence intensity and intracellular localization of the FA transporters, which was analyzed by a confocal immunofluorescence microscopy method (Fig. 2B). Fatty acid transporters in L6 myotubes were dispersed throughout the cell interior and plasma membrane (as visualized by immunostaining, Fig. 2B). More pronounced increase in the staining intensity for fatty acid transporters was observed in the group with post-PA-silencing of ASI60 (PA/ASI60⁻ vs. Ctrl, Fig. 2B).

Effects of pre- and post-PA-silencing of ASI60 on palmitic acid uptake in L6 myotubes

As shown in Figure 3, basal palmitate uptake was increased in PA-treated myotubes (+25%, *P* < 0.05). Correspondingly, the

radioactive palmitate incorporation into the cells was enhanced after ASI60 silencing, with more pronounced changes in the group with post-PA-silencing of ASI60 (ASI60⁻/PA and PA/ASI60⁻ vs. PA: +104% and +212%, respectively, *P* < 0.05, Fig. 3).

Effects of pre- and post-PA-silencing of ASI60 on FFA, DAG, TAG, and PL content and composition in L6 myotubes

To further investigate the effects of ASI60 silencing on cellular fate of palmitate, the intracellular lipid content, fatty acid composition and FA saturation status was assessed.

Free fatty acids. Intramyocellular FFA concentration was raised by palmitate treatment (+45%, PA vs. Ctrl, *P* < 0.05, Fig. 4A) and normalized by pre-PA-silencing of ASI60 (ASI60⁻/PA vs. PA, *P* > 0.05, Fig. 4A). This alteration was mainly caused by the elevation in the content of FFA containing palmitic, palmitoleic, stearic, linoleic, behenic, arachidonic, and nervonic acids after palmitate treatment (PA vs. Ctrl, *P* < 0.05, Table I) and a decrease in the content of unsaturated fatty acids after pre-PA-silencing of ASI60 (ASI60⁻/PA vs. PA, *P* < 0.05, Table I). However, the

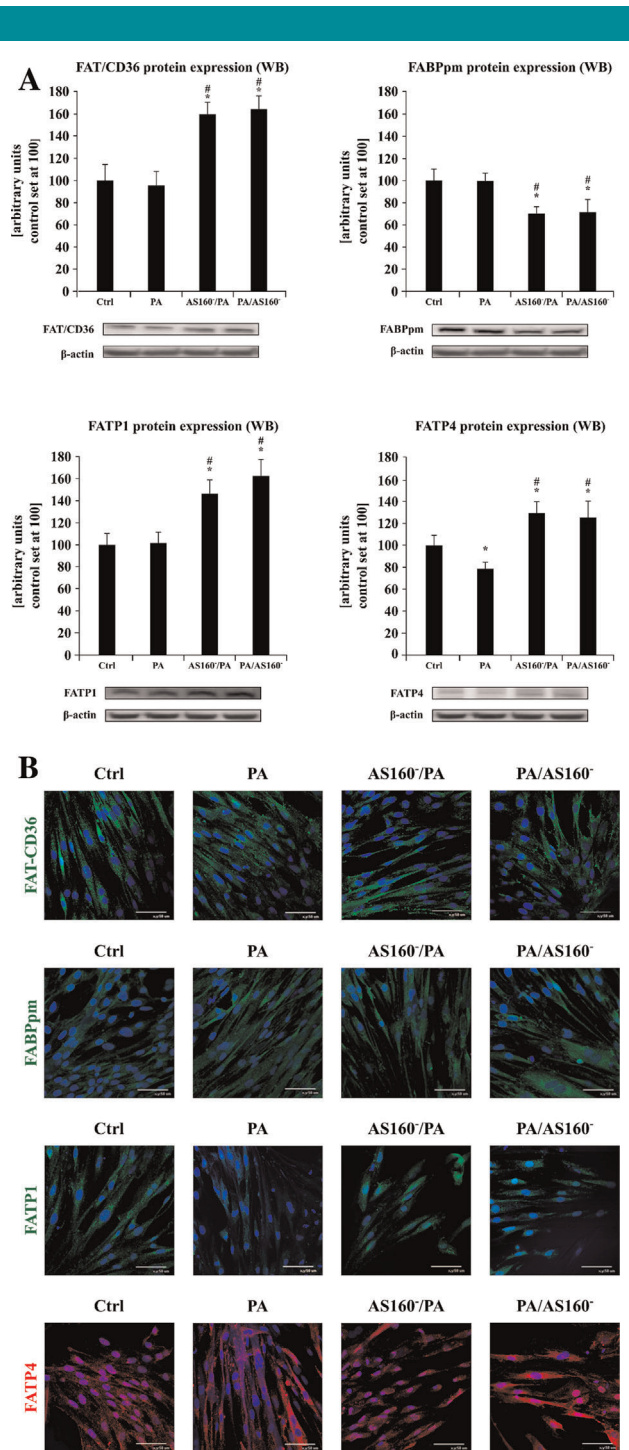


Fig. 2. The effect of pre- and post-PA-silencing of ASI60 on the expression of fatty acid transporters (analyzed by Western Blot [A]) and their localization (investigated by immunofluorescence staining [B]) in L6 myotubes. Data are based on 6 independent determinations for each treatment (bar height = mean, whiskers = SD). Values are expressed in arbitrary units; control group was set as 100. Representative Western blots and immunofluorescence images are shown. ANOVA followed by pairwise Student's *t*-test (with the Holm *P*-value multiplicity correction) was applied. Whenever their assumptions did not hold the Kruskal–Wallis rank test with the subsequent pairwise Wilcoxon test (with the Holm *P*-value multiplicity correction) was conducted. [#]*P* < 0.05 significant difference: control (CTRL) versus treatment. ^{*}*P* < 0.05 significant difference: palmitate (PA) versus treatment.

percentage composition of FFA was virtually the same (Fig. 4B). On the contrary, palmitate incubation with subsequent ASI60 knockdown promoted an increase in total FFA content (PA/ASI60⁻ vs. PA, +45%, *P* < 0.05, Fig. 4A). The contents of FFA containing palmitic, stearic, linolenic, and benenic acid were increased (+32%, +68%, +33%, +43%, *P* < 0.05, Table I) and the contents of palmitoleic and arachidonic acid were decreased (–71%, –21%, *P* < 0.05, Table I). As a result, the percentage share of palmitic acid in the FFA composition decreased, whereas the share of stearic acid increased (PA/ASI60⁻ vs. PA, *P* < 0.05, Fig. 4B).

Diacylglycerols. Similarly, palmitate induced a significant increase in total DAG content (+110%, PA vs. Ctrl, *P* < 0.05, Fig. 5A) and an upward tendency for DAG in the pre-PA-silencing of ASI60 group (ASI60⁻/PA vs. PA, *P* > 0.05, Fig. 5A). In comparison with the control group palmitate treatment elevated DAG content of saturated fatty acids (+176% palmitic, +49% stearic, +125% lignoceric, *P* < 0.05) with accompanying changes in PUFA (+70% linoleic, +100% linolenic, +80% arachidonic, +167% eicosapentaenoic, *P* < 0.05) and MUFA (+438% palmitoleic, *P* < 0.05) (Table II). There were also some changes in the percentage distribution of DAG-constituting fatty acid species. The percentage content of palmitic acid rose, whereas the percentage share of stearic and myristic acids was reduced. On the other hand, the saturation status and percentage content remained unchanged in the group with pre-PA-silencing of ASI60 as compared to the myotubes treated with palmitate alone (Fig. 5B, Table II, *P* > 0.05). Conversely, palmitate treatment with subsequent ASI60 knockdown resulted in a significant decrease in DAG content (PA/ASI60⁻ vs. PA, –28%, *P* < 0.05, Fig. 5A). Post-PA-silencing of ASI60 reduced the content of DAG containing palmitic and palmitoleic, but increased linoleic, linolenic, and nervonic fatty acid content (Table II, *P* < 0.05), this in turn translated into a significant reduction in the saturation status. As a result, the percentage share of palmitic acid in the DAG composition dropped, whereas the share of stearic acid increased (PA/ASI60⁻ vs. PA, *P* < 0.05, Fig. 5B).

Triacylglycerols. Furthermore, as expected palmitate provision led to a substantial (~12-fold) increase in TAG level (Ctrl vs. PA, *P* < 0.05, Fig. 6A). After palmitate treatment the most profound increase was observed for triacylglycerol containing myristic, palmitic, palmitoleic, stearic, oleic, linoleic, arachidonic, lignoceric, and eicosapentaenoic acids (+327%, ~24-fold, ~17-fold, +82%, +126%, +225%, +58%, +131%, and +74%, respectively, PA vs. Ctrl, *P* < 0.05, Table III). Consequently, the percentage content of TAG was changed in such a way that the percentage share of palmitic acid in the TAG composition increased, whereas of the share of myristic, stearic, and oleic acids decreased (PA vs. Ctrl, *P* < 0.05, Fig. 6B). This was reflected in the increase in the amount of saturated TAG with accompanying increase in MUFA and PUFA content (Table III). Interestingly, two different settings, namely pre- and post-PA-silencing of ASI60 showed contrasting impact on TAG content and composition. The content of TAG was basically unaffected by pre-PA-silencing of ASI60, with only modest increase in the content of palmitoleic acid and a decrease in eicosapentaenoic acid (ASI60/PA⁻ vs. PA, +28%, –32%, respectively, *P* < 0.05, Fig. 6A, Table III) as compared to that observed in the PA-treated myotubes. On the other hand, post-PA-silencing of ASI60 had the opposite effect with respect to TAG content, which decreased by 58% (PA/ASI60⁻ vs. PA, *P* < 0.05, Fig. 6A). In that group, the content of TAG containing myristic, palmitic, palmitoleic, oleic, and linoleic acid was diminished, whereas the levels of arachidic, linolenic, lignoceric and eicosapentaenoic acids were significantly elevated (PA/ASI60⁻ vs. PA, *P* < 0.05, Table III). In the case of TAG post-PA-silencing of ASI60 decreased the content of

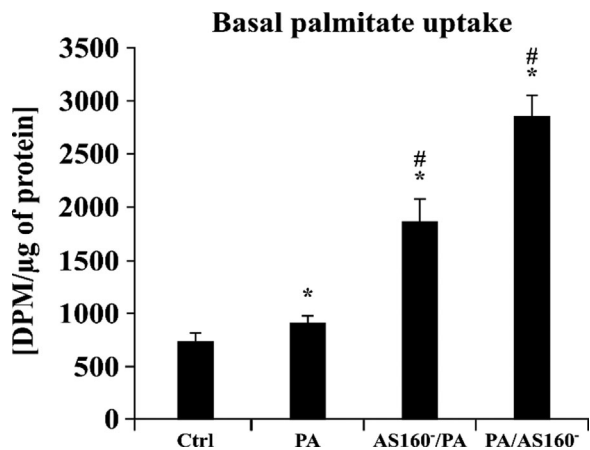


Fig. 3. The effect of pre- and post-PA-silencing of *AS160* on basal palmitate uptake in L6 myotubes. Data are based on 6 independent determinations for each treatment (bar height = mean, whiskers = SD). Values are expressed in arbitrary units; control group was set as 100. ANOVA followed by pairwise Student's *t*-test (with the Holm *P*-value multiplicity correction) was applied. Whenever their assumptions did not hold the Kruskal-Wallis rank test with the subsequent pairwise Wilcoxon test (with the Holm *P*-value multiplicity correction) was conducted. **P* < 0.05 significant difference: control (CTRL) versus treatment, #*P* < 0.05 significant difference: palmitate (PA) versus treatment.

saturated FA with concomitant decrease in MUFA content as compared with the muscle cells incubated with palmitate alone (PA/*AS160*⁻ vs. PA, *P* < 0.05, Table III). Additionally, the percentage share of palmitic and oleic acid in the TAG composition diminished, whereas the share of myristic and palmitoleic acid increased (PA/*AS160*⁻ vs. PA, *P* < 0.05, Fig. 6B).

Phospholipids. Finally, total PL content increased by 89% after palmitate incubation (PA vs. Ctrl, *P* < 0.05, Fig. 7A) and remained unchanged after pre-PA-silencing of *AS160* (*AS160*⁻/PA vs. PA, *P* > 0.05, Fig. 7A). On the other hand, post-PA-silencing of *AS160* significantly reduced PL content (-39%, PA/*AS160*⁻ vs. PA, *P* < 0.05, Fig. 7A). Palmitate treatment increased the amount of saturated fatty acids (palmitic acid +221%, *P* < 0.05, Table IV) and concomitantly increased MUFA (palmitoleic acid +236%, *P* < 0.05, Table IV). Consequently, the percentage composition of PL changed. We noticed an increased percentage share of palmitic acid, whereas the share of stearic, arachidonic, and myristic acids was reduced (PA vs. Ctrl, *P* < 0.05, Fig. 7B). Additionally, a pronounced decrease in the amount of saturated PL was observed in both groups after *AS160* silencing (*AS160*⁻/PA, PA/*AS160*⁻ vs. PA, *P* < 0.05, Table IV) with a parallel decrease in MUFA, but only in the case of PA/*AS160*⁻ group which was mainly caused by diminished content of PL containing palmitoleic and oleic fatty acids (-67%, -30%, respectively, *P* < 0.05, Table IV). This was caused by a decrease in the percentage amount of PL containing stearic (*AS160*⁻/PA vs. PA, *P* < 0.05, Fig. 7B), palmitic, and oleic acid (PA/*AS160*⁻ vs. PA, *P* < 0.05, Fig. 7B) as well as by increases in the content of oleic (*AS160*⁻/PA vs. PA, *P* < 0.05, Fig. 7B), stearic and arachidonic acids (PA/*AS160*⁻ vs. PA, *P* < 0.05, Fig. 7B).

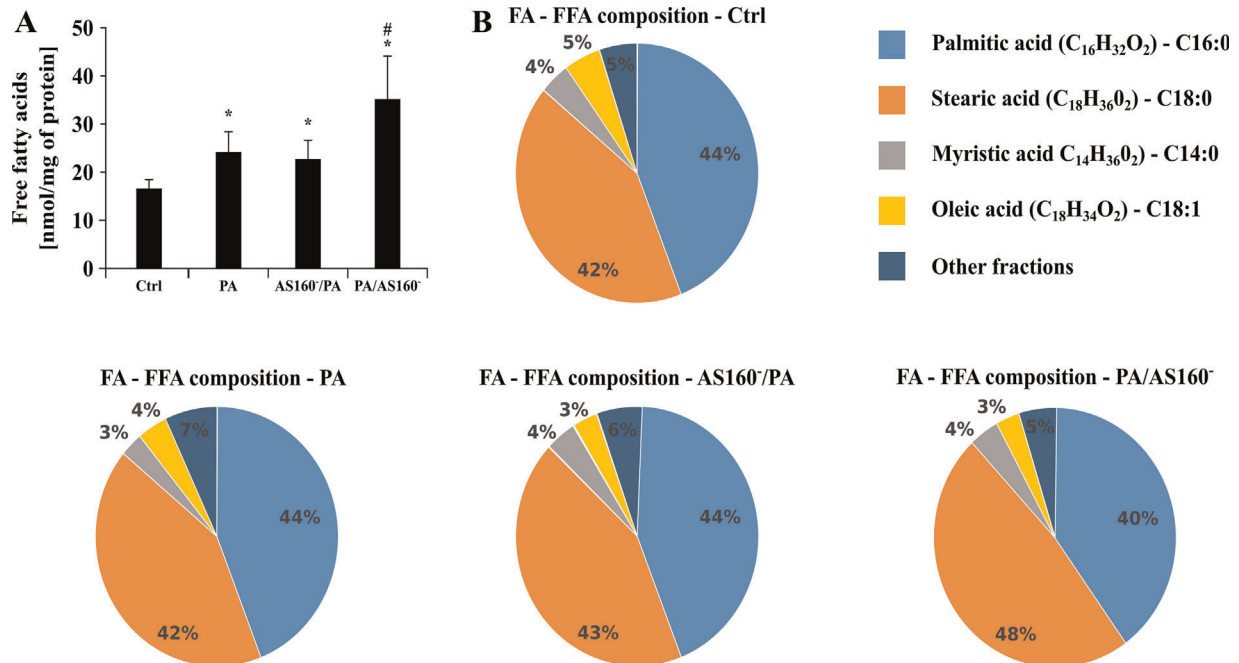


Fig. 4. The effect of pre- and post-PA-silencing of *AS160* on the FFA total content (A) and percentage composition of the most common FA (B) in L6 myotubes. Data are based on 8 independent determinations for each treatment (bar height = mean, whiskers = SD). Values are expressed in nmol mg⁻¹ of protein for total FFA content and nmol % for percentage share of the most frequent FA. ANOVA followed by pairwise Student's *t*-test (with the Holm *P*-value multiplicity correction) was applied. Whenever their assumptions did not hold the Kruskal-Wallis rank test with the subsequent pairwise Wilcoxon test (with the Holm *P*-value multiplicity correction) was conducted. **P* < 0.05 significant difference: control (CTRL) versus treatment, #*P* < 0.05 significant difference: palmitate (PA) versus treatment.

TABLE I. Fatty acid—FFA composition

Acid	Ctrl	PA	ASI60 ⁻ /PA	PA/ASI60 ⁻
Myristic (14:0)	0.88 ± 0.154	0.83 ± 0.206	0.91 ± 0.124	1.37 ± 0.39
Palmitic (16:0)	6.94 ± 0.902	10.77 ± 1.73*	10.03 ± 1.093*	14.25 ± 3.02 [#]
Palmitoleic (16:1)	0.12 ± 0.034	0.48 ± 0.065*	0.43 ± 0.017*	0.14 ± 0.024 [#]
Stearic (18:0)	7.35 ± 0.655	10.14 ± 2.197*	9.92 ± 2.505*	17.00 ± 5.190 [#]
Oleic (18:1n9c)	0.7 ± 0.227	0.91 ± 0.194	0.61 ± 0.064 [#]	0.98 ± 0.116
Linoleic (18:2n6c)	0.26 ± 0.036	0.48 ± 0.129*	0.38 ± 0.15	0.63 ± 0.191*
Arachidic (20:0)	0.22 ± 0.161	0.24 ± 0.053	0.21 ± 0.064	0.39 ± 0.121
Linolenic (C18n3)	0.05 ± 0.025	0.09 ± 0.014	0.12 ± 0.2	0.12 ± 0.026 [#]
Behenic (22:0)	0.04 ± 0.008	0.07 ± 0.01*	0.05 ± 0.009 [#]	0.1 ± 0.02 [#]
Arachidonic (20:4n6)	0.11 ± 0.025	0.14 ± 0.01*	0.09 ± 0.023 [#]	0.11 ± 0.023 [#]
Lignoceric (24:0)	0.02 ± 0.01	0.04 ± 0.013	0.02 ± 0.007	0.04 ± 0.011
Eicosapentaenoic (20:5n3)	0.02 ± 0.008	0.03 ± 0.005	0.02 ± 0.009	0.05 ± 0.009*
Nervonic (24:1)	0.03 ± 0.01	0.06 ± 0.009*	0.03 ± 0.005 [#]	0.07 ± 0.01*
Docosahexaenoic (22:6n3)	Nd.	0.03 ± 0.01	Nd.	0.03 ± 0.012
SAT	15.46 ± 1.554	22.1 ± 4.123*	21.16 ± 3.709*	33.18 ± 8.691 [#]
UNSAT	1.29 ± 0.268	2.2 ± 0.365*	1.68 ± 0.227 [#]	2.1 ± 0.327*
Total	16.74 ± 1.692	24.3 ± 4.178*	22.84 ± 3.849*	35.28 ± 8.992 [#]

The values (nmol mg⁻¹ of protein) are expressed as: mean ± SD; Nd., not detected.
 *P < 0.05, difference versus Ctrl.
[#]P < 0.05, difference versus PA.

Effects of pre- and post-PA-silencing of ASI60 on the expression of mitochondrial proteins (COX IV, CS, and β-HAD) in L6 myotubes

Interestingly, only post-PA-silencing of ASI60 was associated with an increase in β-HAD expression indicating a rise in fatty acids β-oxidation (+38%, PA/ASI60⁻ vs. PA, P < 0.05, Fig. 8C). In addition to the elevated β-HAD level, also enhanced expression of COX IV was observed (+110%, PA/ASI60⁻ vs. PA, P < 0.05, Fig. 8A). Furthermore, we have estimated the expression of citrate synthase considered to be a pace-making enzyme in the citric acid cycle (tricarboxylic acid cycle, TCA) as

well as biomarker for the presence of intact mitochondria. Interestingly, CS content did not significantly differ amongst the groups and only a tendency toward a reduction was observed in the case of post-PA-silencing and silenced alone groups (PA/ASI60⁻ vs. PA and ASI60⁻ vs. Ctrl, P > 0.05, Fig. 8B).

Effects of pre- and post-PA-silencing of ASI60 on the pAkt/Akt ratio in L6 myotubes

The Akt, also known as protein kinase B, is an important protein involved in many physiological processes including insulin signaling,

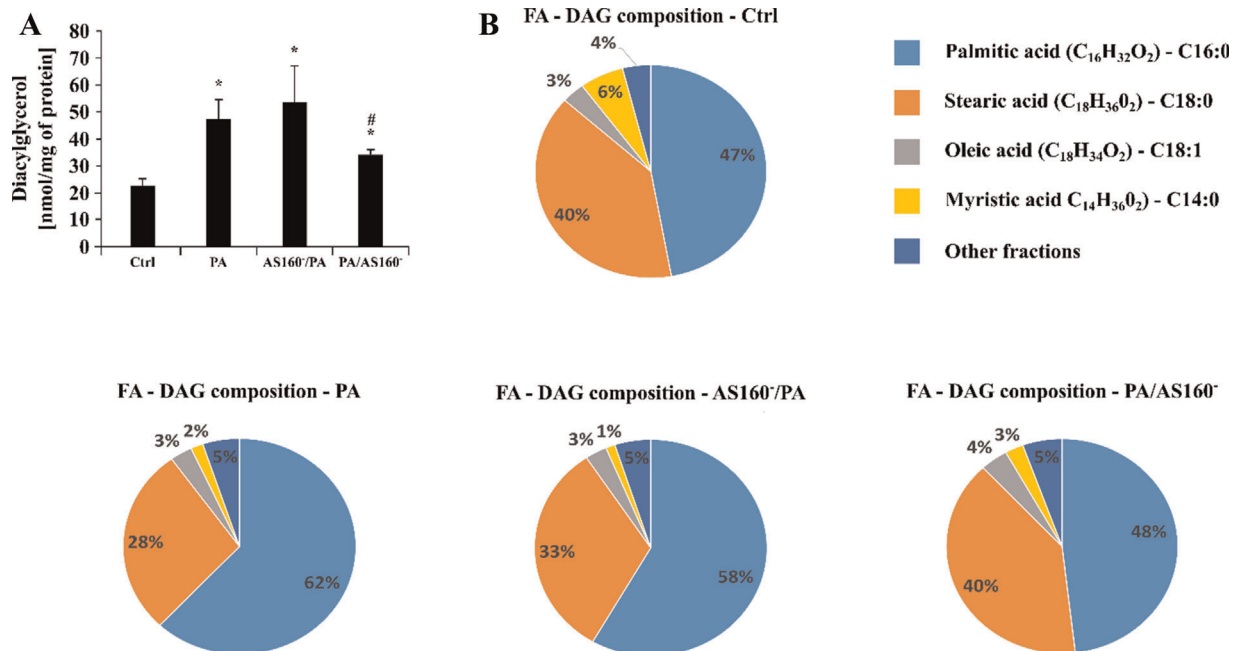


Fig. 5. The effect of pre- and post-PA-silencing of ASI60 on the DAG total content (A) and percentage composition of the most common FA (B) in L6 myotubes. Data are based on 8 independent determinations for each treatment (bar height = mean, whiskers = SD). Values are expressed in nmol mg⁻¹ of protein for total DAG content and nmol % for percentage share of the most frequent FA. ANOVA followed by pairwise Student's t-test (with the Holm P-value multiplicity correction) was applied. Whenever their assumptions did not hold the Kruskal–Wallis rank test with the subsequent pairwise Wilcoxon test (with the Holm P-value multiplicity correction) was conducted. *P < 0.05 significant difference: control (CTRL) versus treatment, [#]P < 0.05 significant difference: palmitate (PA) versus treatment.

TABLE II. Fatty acid—DAG composition

Acid	Ctrl	PA	ASI60 ⁻ /PA	PA/ASI60 ⁻
Myristic (14:0)	1.4 ± 0.955	1.47 ± 0.229	1.62 ± 0.453	1.32 ± 0.153
Palmitic (16:0)	10.66 ± 1.568	29.43 ± 4.846*	31.2 ± 6.693*	16.39 ± 0.849* [#]
Palmitoleic (16:1)	0.21 ± 0.12	1.13 ± 0.122*	1.33 ± 0.174* [#]	0.37 ± 0.06* [#]
Stearic (18:0)	8.93 ± 0.767	13.33 ± 2.061*	17.31 ± 6.132*	13.57 ± 1.044*
Oleic (18:1n9c)	0.73 ± 0.483	0.82 ± 0.074	0.7 ± 0.092	0.88 ± 0.056
Linoleic (18:2n6c)	0.23 ± 0.118	0.39 ± 0.099*	0.39 ± 0.112	0.49 ± 0.056* [#]
Arachidic (20:0)	0.12 ± 0.066	0.25 ± 0.139	0.33 ± 0.148*	0.3 ± 0.024*
Linolenic (C18n3)	0.03 ± 0.014	0.06 ± 0.016*	0.05 ± 0.008* [#]	0.08 ± 0.008* [#]
Behenic (22:0)	0.04 ± 0.024	0.06 ± 0.018	0.06 ± 0.013	0.09 ± 0.026*
Arachidonic (20:4n6)	0.1 ± 0.057	0.18 ± 0.012*	0.16 ± 0.032	0.14 ± 0.042
Lignoceric (24:0)	0.08 ± 0.039	0.18 ± 0.041*	0.16 ± 0.098	0.24 ± 0.047*
Eicosapentaenoic (20:5n3)	0.03 ± 0.009	0.08 ± 0.018*	0.05 ± 0.014* [#]	0.08 ± 0.014*
Nervonic (24:1)	0.05 ± 0.032	0.06 ± 0.01	0.04 ± 0.012	0.08 ± 0.009* [#]
Docosahexaenoic (22:6n3)	Nd.	0.03 ± 0.004	0.1 ± 0.09 [#]	Nd.
SAT	21.2 ± 2.085	44.61 ± 6.972*	50.56 ± 13.269*	31.75 ± 1.888* [#]
UNSAT	1.41 ± 0.779	2.88 ± 0.259*	2.93 ± 0.405*	2.28 ± 0.146* [#]
Total	22.61 ± 2.437	47.49 ± 6.866*	53.5 ± 13.432*	34.04 ± 1.948* [#]

The values (nmol mg⁻¹ of protein) are expressed as: mean ± SD; Nd., not detected.

**P* < 0.05, difference versus Ctrl.

[#]*P* < 0.05, difference versus PA.

protein synthesis, and ASI60 activation. In the following study we assessed pAkt/Akt ratio, which is a measure of Akt activity. Interestingly, pAkt/Akt ratio was increased by 23% in ASI60⁻ silenced myotubes (ASI60⁻ vs. Ctrl, *P* < 0.05, Fig. 9), but decreased after palmitate incubation (-40%, PA vs. Ctrl, *P* < 0.05, Fig. 9). Moreover, it seems that both pre- and post-PA-silencing of ASI60 significantly boosted the activity of Akt (ASI60⁻/PA and PA/ASI60⁻ vs. PA; +68% and +43%, respectively, *P* < 0.05, Fig. 9).

Discussion

The current study compared for the first time the effects of pre- and post-PA-silencing of ASI60 (groups designations:

ASI60⁻/PA and PA/ASI60, respectively) on lipid status in L6 myotubes. We found that palmitate incubation together with subsequent ASI60 knockdown resulted in marked decrements in the content of DAG, TAG and PL lipid fractions, but also in an increased FFA content. These changes were accompanied by pronounced decreases in the amount of saturated fatty acids (SFAs) composing TAG and PL lipid fractions with decreased proportion of MUFA species as compared to palmitate alone (PA/ASI60⁻ vs. PA). Interestingly, the opposite effect was observed for a group with pre-PA-silencing of ASI60, in which we did not notice any statistically significant differences with respect to the examined lipid pools contents. Furthermore, in the present study we revealed (via immunoblotting method)

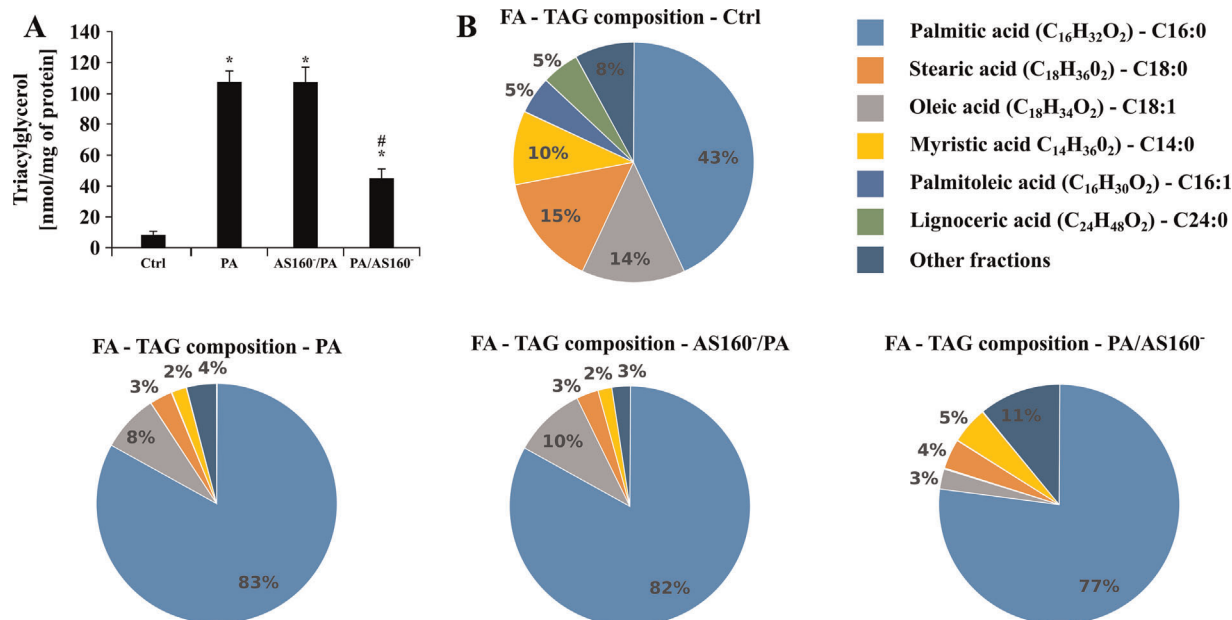


Fig. 6. The effect of pre- and post-PA-silencing of ASI60 on the TAG total content (A) and percentage composition of the most common FA (B) in L6 myotubes. Data are based on 8 independent determinations for each treatment (bar height = mean, whiskers = SD). Values are expressed in nmol mg⁻¹ of protein for total TAG content and nmol % for percentage share of the most frequent FA. ANOVA followed by pairwise Student's *t*-test (with the Holm *P*-value multiplicity correction) was applied. Whenever their assumptions did not hold the Kruskal–Wallis rank test with the subsequent pairwise Wilcoxon test (with the Holm *P*-value multiplicity correction) was conducted. **P* < 0.05 significant difference: control (CTRL) versus treatment, [#]*P* < 0.05 significant difference: palmitate (PA) versus treatment.

TABLE III. Fatty acid—TAG composition

Acid	Ctrl	PA	ASI60 ⁻ /PA	PA/ASI60 ⁻
Myristic (14:0)	0.85 ± 0.217	3.63 ± 0.448*	3.09 ± 0.681*	1.88 ± 0.32* [#]
Palmitic (16:0)	3.58 ± 0.992	88.56 ± 7.256*	88.67 ± 8.443*	34.79 ± 5.26* [#]
Palmitoleic (16:1)	0.46 ± 0.058	8.06 ± 1.071*	10.31 ± 0.97* [#]	1.21 ± 0.171* [#]
Stearic (18:0)	1.27 ± 0.516	2.31 ± 0.276*	1.9 ± 0.492	2.21 ± 0.232*
Oleic (18:1n9c)	1.16 ± 0.385	2.62 ± 0.358*	2.33 ± 0.219*	2.02 ± 0.207* [#]
Linoleic (18:2n6c)	0.08 ± 0.071	0.26 ± 0.088*	0.15 ± 0.082	0.08 ± 0.077* [#]
Arachidic (20:0)	0.06 ± 0.022	0.08 ± 0.016	0.08 ± 0.021	0.15 ± 0.073* [#]
Linolenic (C18n3)	0.09 ± 0.045	0.09 ± 0.064	0.06 ± 0.047	0.18 ± 0.059* [#]
Behenic (22:0)	Nd.	0.02 ± 0.024	0.01 ± 0.021	Nd.
Arachidonic (20:4n6)	0.12 ± 0.016	0.19 ± 0.028*	0.17 ± 0.062	0.19 ± 0.062
Lignoceric (24:0)	0.39 ± 0.189	0.9 ± 0.366*	0.46 ± 0.308	1.65 ± 0.544* [#]
Eicosapentaenoic (20:5n3)	0.34 ± 0.042	0.59 ± 0.045*	0.4 ± 0.071* [#]	0.8 ± 0.133* [#]
Nervonic (24:1)	0.01 ± 0.027	0.03 ± 0.025	0 ± 0.003	0.02 ± 0.034
Docosahexaenoic (22:6n3)	Nd.	Nd.	Nd.	Nd.
SAT	5.77 ± 1.661	94.62 ± 7.355*	93.76 ± 8.932*	39.05 ± 5.5* [#]
UNSAT	2.65 ± 0.7	12.7 ± 1.374*	13.88 ± 1.356*	6.12 ± 0.917* [#]
Total	8.42 ± 2.147	107.32 ± 7.411*	107.64 ± 9.647*	45.17 ± 5.979* [#]

The values (nmol mg⁻¹ of protein) are expressed as: mean ± SD; Nd., not detected.
 *P < 0.05, difference versus Ctrl.
[#]P < 0.05, difference versus PA.

that pre- and post-silencing of ASI60 combined with palmitate treatment increased the total expression of most of the examined fatty acid transporters, namely: FAT/CD36, FATP-1, 4, but decreased the level of FABPpm. As an additional confirmation of the results, we visualized intracellular and sarcolemmal localization of FA transporters using immunofluorescence staining.

It is well known that upon insulin stimulation ASI60 is phosphorylated on a number of Akt consensus sequences, this in turn leads to an inactivation of its Rab-GAP activity. As a result GSV-associated Rabs are loaded with GTP and this leads to translocation of GLUT4 to the plasma membrane (Fig. 10) (Sakamoto and Holman, 2008). Direct examination of 3T3-L1

adipocytes showed that the presence of ASI60-4P, a mutant form in which four of the phosphorylation sites amino acids (Ser318, Ser588, Thr642, Ser751) had been replaced with alanine, significantly reduced insulin-stimulated GLUT4 translocation to the cell surface (Sano et al., 2003). Accordingly, numerous studies in humans and rodents corroborate that insulin-stimulated ASI60 phosphorylation is diminished in insulin resistant state and in type 2 diabetes (Vind et al., 2011; Karlsson et al., 2005). In contrast to the strong evidence linking ASI60 to insulin-stimulated glucose transport, the evidence for the role of this protein in fatty acid induced insulin resistance is scarcer and less conclusive (Fig. 10). To date, the effects of ASI60 knockdown on protein-mediated

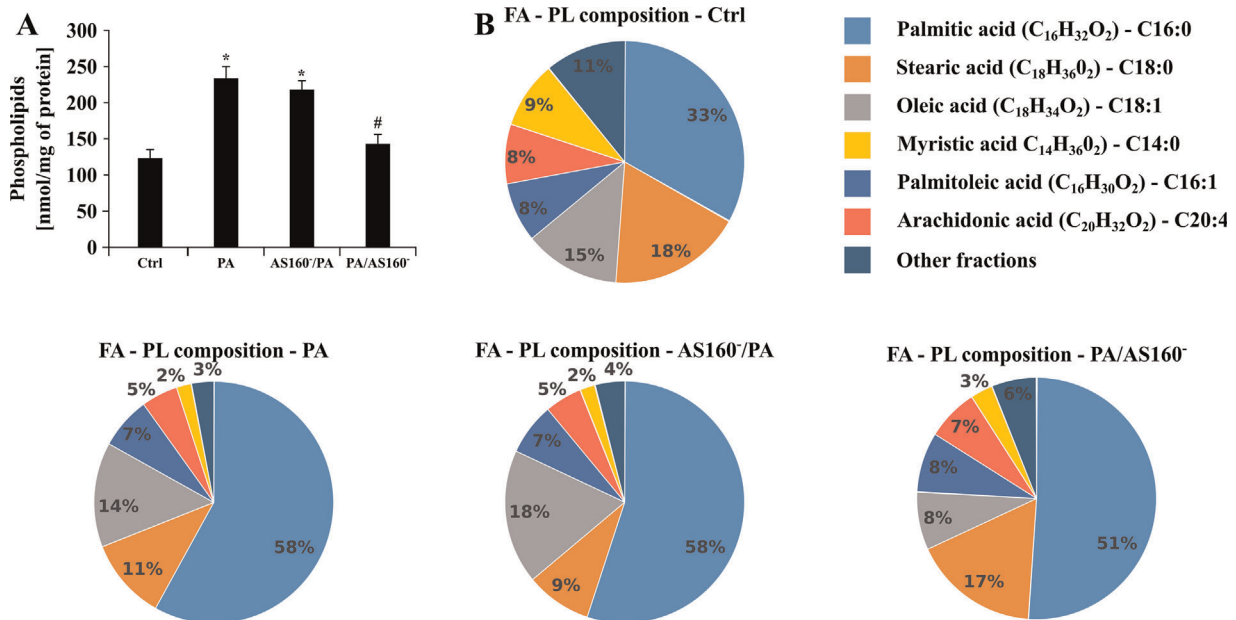


Fig. 7. The effect of pre- and post-PA-silencing of ASI60 on the PL total content (A) and percentage composition of the most common FA (B) in L6 myotubes. Data are based on 8 independent determinations for each treatment (bar height = mean, whiskers = SD). Values are expressed in nmol mg⁻¹ of protein for total PL content and nmol % for percentage share of the most frequent FA. ANOVA followed by pairwise Student's t-test (with the Holm P-value multiplicity correction) was applied. Whenever their assumptions did not hold the Kruskal-Wallis rank test with the subsequent pairwise Wilcoxon test (with the Holm P-value multiplicity correction) was conducted. *P < 0.05 significant difference: control (CTRL) versus treatment, [#]P < 0.05 significant difference: palmitate (PA) versus treatment.

TABLE IV. Fatty acid—PL composition

Acid	Ctrl	PA	ASI60 ⁻ /PA	PA/ASI60 ⁻
Myristic (14:0)	10.67 ± 1.75	5.22 ± 0.571*	4.35 ± 0.573* [#]	4.06 ± 0.582* [#]
Palmitic (16:0)	40.9 ± 7.442	131.33 ± 15.221*	115.95 ± 9.292* [#]	68.59 ± 8.676* [#]
Palmitoleic (16:1)	9.78 ± 0.845	32.83 ± 2.983*	39 ± 1.987* [#]	10.97 ± 1.985* [#]
Stearic (18:0)	22.16 ± 2.861	24.75 ± 3.155	19.17 ± 0.825* [#]	23.43 ± 2.33
Oleic (18:1n9c)	15.59 ± 1.641	14.85 ± 1.073	14.5 ± 0.836	10.41 ± 1.648* [#]
Linoleic (18:2n6c)	8.82 ± 1.063	7.74 ± 0.42	7.83 ± 0.504	8.4 ± 1.228
Arachidic (20:0)	0.4 ± 0.102	0.32 ± 0.109	0.4 ± 0.117	0.57 ± 0.151* [#]
Linolenic (C18n3)	0.23 ± 0.451	Nd.	0.78 ± 0.358*	Nd.
Behenic (22:0)	Nd.	Nd.	Nd.	Nd.
Arachidonic (20:4n6)	10.39 ± 1.175	10.92 ± 0.756	11.4 ± 0.653	8.92 ± 1.468* [#]
Lignoceric (24:0)	1.26 ± 1.051	1.71 ± 0.566	0.78 ± 0.097* [#]	3.07 ± 0.928* [#]
Eicosapentaenoic (20:5n3)	1.91 ± 0.301	2.14 ± 0.211	2.05 ± 0.099	2.43 ± 0.5
Nervonic (24:1)	Nd.	Nd.	Nd.	Nd.
Docosahexaenoic (22:6n3)	1.49 ± 0.312	1.59 ± 0.446	1.64 ± 0.202	2.08 ± 0.365
SAT	74.14 ± 11.918	161.61 ± 18.249*	139.88 ± 9.793* [#]	96.66 ± 10.221* [#]
UNSAT	49.47 ± 4.206	71.8 ± 4.972*	77.98 ± 4.184*	46.29 ± 7.285* [#]
Total	123.6 ± 12.06	233.41 ± 21.081*	217.86 ± 12.904*	142.95 ± 17.088* [#]

The values (nmol mg⁻¹ of protein) are expressed as: mean ± SD; Nd., not detected.

**P* < 0.05, difference versus Ctrl.

[#]*P* < 0.05, difference versus PA.

LCFA transport into skeletal muscle have not been examined in insulin resistant state. In the present study fatty acid transporters content was estimated in the whole muscle cells extracts using Western blotting and additionally immunofluorescence microscopy method was used to determine immunofluorescence intensity and proteins localization in the skeletal muscle cells. It is well known that

immunofluorescence is a valuable technique that can provide (semi)quantitative data as well as yield informative images showing the localization of the proteins of interest (Bradley et al., 2014). In our previous paper, we demonstrated that in normal conditions in L6 myotubes moderate silencing of ASI60 increased the total expression of FAT/CD36 and FABPpm, and did not change FATP-I and 4 contents (Miklosz et al., 2016).

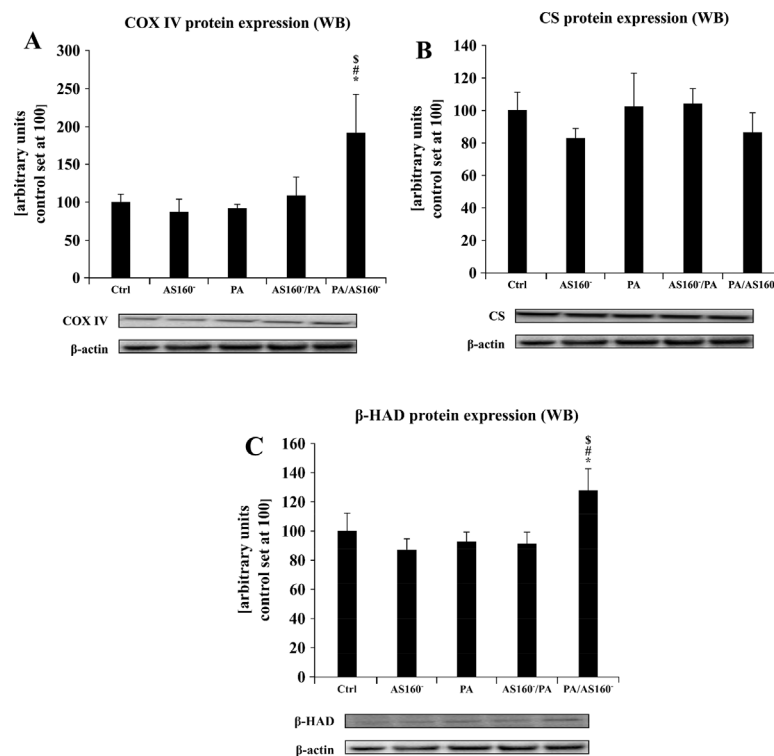


Fig. 8. The effect of pre- and post-PA-silencing of ASI60 on the expression of total expression of mitochondrial proteins: COX IV (A), CS (B), and β -HAD (C) in L6 myotubes. Data are based on 6 independent determinations for each treatment (bar height = mean, whiskers = SD). Values are expressed in arbitrary units; control group was set as 100%. Representative Western blot images are shown. ANOVA followed by pairwise Student's *t*-test (with the Holm *P*-value multiplicity correction) was applied. Whenever their assumptions did not hold the Kruskal-Wallis rank test with the subsequent pairwise Wilcoxon test (with the Holm *P*-value multiplicity correction) was conducted. **P* < 0.05 significant difference: control (CTRL) versus treatment, [#]*P* < 0.05 significant difference: palmitate (PA) versus treatment, ^S*P* < 0.05 significant difference: knockdown of ASI60 (ASI60⁻) versus treatment.

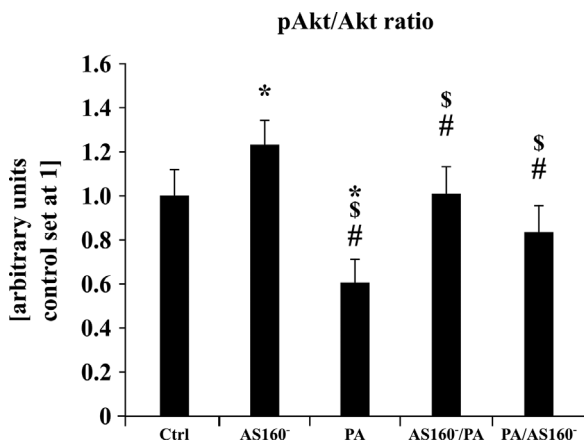


Fig. 9. The effect of pre- and post-PA-silencing of ASI60 on the ratio of pAkt/Akt in L6 myotubes. Data are based on 6 independent determinations for each treatment (bar height = mean, whiskers = SD). Control group was set as 100%. Representative Western blots images are shown. ANOVA followed by pairwise Student's *t*-test (with the Holm *P*-value multiplicity correction) was applied. Whenever their assumptions did not hold the Kruskal–Wallis rank test with the subsequent pairwise Wilcoxon test (with the Holm *P*-value multiplicity correction) was conducted. **P* < 0.05 significant difference: control (CTRL) versus treatment, #*P* < 0.05 significant difference: palmitate (PA) versus treatment.

The data presented herein demonstrate that pre- and post-silencing of ASI60 combined with palmitate treatment increased the expression of fatty acid transporters, namely: FAT/CD36, FATP-1, 4, but not FABPpm. In skeletal muscles, long chain fatty acid transporters: FAT/CD36, FABPpm, FATP-1, 4 are co-expressed. It is well known that each of the transporters may increase fatty acid transport, though FAT/CD36 and FATP-4 are the most effective ones, whereas FAT/CD36 and FABPpm are key players stimulating fatty acid

oxidation (Nickerson et al., 2009). Furthermore, there is also evidence that in insulin resistant state as well as in type I and II diabetes, some fatty acid transporters (i.e., FAT/CD36, FATP-1, 4, but not FABPpm) are involved in the dysregulation of fatty acid metabolism in skeletal muscle tissue (Bonen et al., 2004). Currently, we showed that the expressions of FAT/CD36 and FATP-1, 4 have been upregulated in both settings of our experiment (i.e., pre- and post-PA-silencing of ASI60), which indicates a crucial role of ASI60 in altering fatty acid transport into myocytes (Fig. 10). This is also in concordance with the observed intensified palmitic acid uptake into the muscle cells, which suggests that silencing of ASI60 favors subsequent intracellular influx of palmitate into L6 myotubes. It is also known that fatty acid transporters content is highly coupled with FA transport. This phenomenon was observed in human breast cancer (Schimanski et al., 2010) and also in uterine fibroids (Knapp et al., 2016) with diminished FA transport proteins expression, which resulted in decreased FA transport into these cells. With regards to the potential mechanism of how ASI60 knockdown could lead to an increase in the protein expression of FA transporters. Firstly, in our study the expression of Akt (more specifically the ratio of phosphoAkt/Akt, a measure of Akt activity), which is an upstream molecule for ASI60, was increased after ASI60 knock down (either alone or combined with palmitate incubation). Since it is known that Akt can stimulate protein synthesis (Enomoto et al., 2005), the observed increase in the total expression level of fatty acid transporters might be a result of enhanced Akt activity. The observed increase in the total expression of fatty acid transporters might be a result of the enhanced Akt activity. Secondly, immunofluorescence microscopy was used to determine fatty acid proteins intracellular localization. In the basal condition (in the presented study) FA transporters were dispersed throughout the cell interior and plasma membrane. Thirdly, PI3K/Akt pathway acts as a signaling network rather than a single linear cascade, in which multiple interactions and feedback loops exist (Wong et al., 2016). Therefore, it is also possible that ASI60 activity might have been regulated (mutual interactions with different molecules) at multiple levels, rather than in a simple linear fashion (Roberts and Der, 2007). However, the mechanistic basis for this phenomenon remains

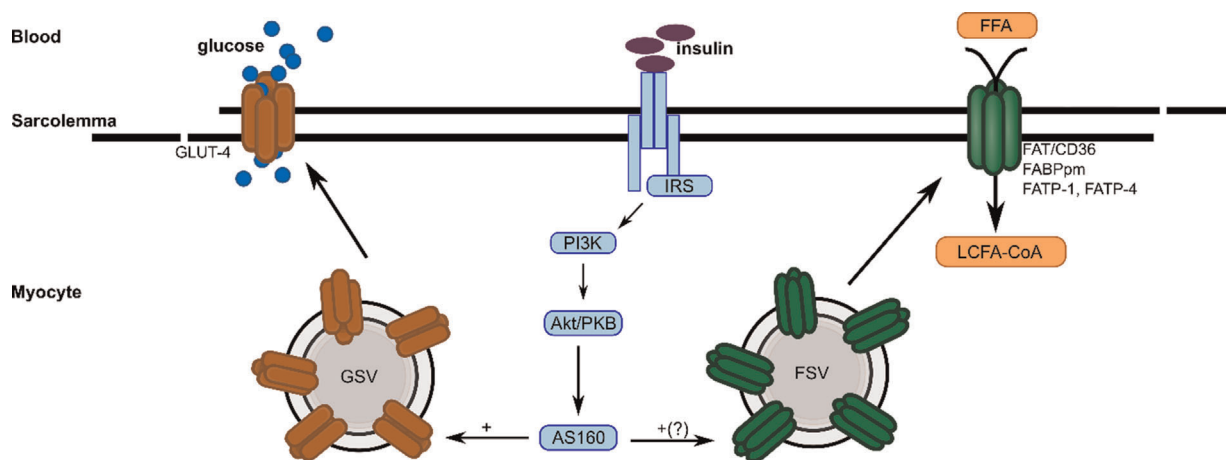


Fig. 10. The effects of ASI60 actions on glucose and fatty acid transport into myocytes. Akt/PKB—protein kinase B; ASI60—Akt substrate of 160 kDa; FABPpm—plasma membrane associated fatty acid binding protein; FAT/CD36—fatty acid translocase/cluster of differentiation 36; FATP-1,4—fatty acid transport proteins 1 and 4; FFA—free fatty acids; FSV—fatty acid transporters storage vesicles; GLUT4—glucose transporter type 4; GSV—glucose transporters (GSV) storage vesicles; IRS—insulin receptor substrate; LCFA-CoA—long chain fatty acid acyl-CoA; PI3K—phosphatidylinositol-4,5-bis-phosphate 3-kinase.

to be further explored. Summing up, we can postulate that after ASI60 knock down the plasmalemmal expression of FA transporters should be higher. If so, then the lack of ASI60 Rab GAP function in the ASI60 silenced myocytes most likely leads to an increased amount of GTP-bound Rabs that in turn trigger unrestricted FA transporters translocation to the plasma membrane (Lansey et al., 2012). In line with these notions, Samovski et al. (2012) have recently confirmed that in cardiomyocytes the GTP-bound Rab8a protein, which is under ASI60 control, regulates FAT/CD36 trafficking to the plasma membrane. In that study a 70% decrease in the expression of ASI60 protein resulted in a 2.5-fold increase in the surface FAT/CD36 expression, with no evident changes in the total protein level (Samovski et al., 2012). We, on the other hand, did not observe any significant changes with respect to lipid content (ASI60⁻/PA vs. PA) despite the enhanced FA transporters expression and increased palmitate acid uptake. Interestingly, our intervention (post-PA-silencing of ASI60 group) resulted in lower intramyocellular TAG, DAG, and PL levels accompanied by an increment in the amount of FFA. Therefore, we may speculate that the ASI60 knockdown combined with palmitate treatment had, probably, led to an enhanced rate of fatty acid oxidation in L6 myotubes as confirmed by the increased levels of COX IV and β -HAD proteins (Fig. 8). Nonetheless, we should be aware that the myocellular lipid content does not exactly reflect the processes of FA oxidation or esterification in the muscle cells (Dyck et al., 2001). Finally, it is also possible, that the impact of modest ASI60 knockdown (~25% decrease in its protein level presented in our study) could have been compensated by the residual RabGAP activity exerted (Chadt et al., 2015). Therefore, in order to support the non-redundant roles for the two Rab GAPs proteins, TBCID1 expression level has been assessed. TBCID1 (a paralog of TBCID4) protein expression was the same in all of the studied groups, indicating constant presence of TBCID1 throughout the experiments. Thus, it seems that TBCID1 expression does not compensate for the lack of ASI60. Moreover, these results correspond to those reported by Lansey et al. (2012) who had previously found no change in the level of TBCID1 in ASI60^{-/-} skeletal muscle and adipose tissue. Additionally, Szekeres et al. (2012) has also reported no up-regulation of ASI60 in TBCID1-deficient skeletal muscles. This indicates that both Rab GAP proteins operate to a large extent separately and do not compensate for the loss of their counterpart.

So far, most of the studies suggest that the level of circulating free fatty acids is markedly increased in insulin-resistant conditions such as obesity and type 2 diabetes (T2DM) (Consitt et al., 2009). The augmented entry of FFA into myocytes without an equivalent elevation in lipid oxidation, contributes to the accumulation of intramyocellular lipids, which are involved in the development of skeletal muscle insulin resistance. Amongst different types of fatty acids palmitic and stearic acid were found to be the most potent inducers of insulin resistance (Martins et al., 2012) in skeletal muscle cells in general (Coll et al., 2008; Yuzefovych et al., 2010) and in muscles of animals fed with high fat diet (Lee et al., 2006). In accordance with our expectations we showed that palmitate provision results in excessive accumulation of intramyocellular lipids, that is, FFA, DAG, TAG, and PL, which was caused by the observed elevation in the level of saturated fatty acid species. As mentioned above, palmitate one of the most abundant fatty acids in FA fraction is an important precursor of de novo synthesis of ceramide, which inhibits insulin action in muscle cells (Gao et al., 2009). Moreover, evidence from the various previously conducted studies confirm that the prolonged exposure of skeletal muscle cells to palmitate increases also DAG level, which subsequently activates the PKC θ -NF κ B route that disrupts the insulin signaling pathway (Coll et al., 2008). Furthermore, it is widely accepted that poly- (e.g., linoleate) and monounsaturated

(e.g., oleate) fatty acids are more readily oxidized than their saturated counterparts (e.g., palmitate and stearate), thus potentially contributing to the excessive accumulation of more harmful lipid fractions (DeLany et al., 2000; Gaster et al., 2005). However, the role of ASI60 in the fatty acid induced insulin resistance remains poorly explored. To date, it seems that only one research (our own previous study) has demonstrated that ASI60 modulation may induce changes with respect to lipid content and composition in L6 myotubes (Miklosz et al., 2016). In the aforementioned research, we showed that modest, temporary knockdown of ASI60 (-25% of protein content) caused increased contents of DAG and PL, which was mainly due to the elevation of saturated fatty acid lipid species. On the contrary, we observed a decrease in the amount of TAG caused by a reduction in the palmitate and stearate acids levels (Miklosz et al., 2016). The data presented herein showed that pre- and post-silencing of ASI60 combined with the palmitate treatment had different impact on lipid pool(s) when compared with the palmitate group alone. Interestingly, pre-PA-silencing of ASI60 had virtually no effect on intramyocellular lipid concentration (ASI60⁻/PA vs. PA), whereas post-PA-silencing of ASI60 induced even more pronounced accumulation with respect to FFA content, but reduced other lipid fractions level (i.e., DAG, TAG, and PL) (PA/ASI60⁻ vs. PA). Here, in the group with post-PA-silencing of ASI60, we observed a significant increase in FA saturation status in the case of FFA. The above was probably caused by increased concentrations of palmitic, stearic and behenic fatty acid species. Indeed, it is generally accepted that saturated fatty acids have been implicated in the development of insulin resistance, whereas MUFAs and PUFAs have less pronounced effect or even (at least in some instances) can improve insulin sensitivity in skeletal muscle (Dimopoulos et al., 2006; Coll et al., 2008). The accumulation of FFA in myocytes might result from an imbalance between FFA uptake, the rate/magnitude of their storage into TAG pool and/or their mitochondrial oxidation. A number of studies in obese humans and high fat-fed rats revealed that an enhanced transport of FA into skeletal muscle tissue is associated with an increased IMTG content, which exerts an adverse effect on the tissue's insulin sensitivity (Hegarty et al., 2002; Bonen et al., 2004). Consistently with this reports, we have also noticed intensified FA transport into myocytes, which was clearly visible in the case of increased basic palmitate acid uptake, although it was not reflected in the accumulation of TAG. Our data demonstrate that pre-incubation with palmitate (PA/ASI60-group) caused an increased influx of FA that in turn enhanced mitochondrial β -oxidation (fatty acids, for instance, are known to activate PPARs) which would result in less potent FA esterification/accumulation afterwards. In accordance with this notion, mitochondrial proteins expression was significantly increased (COX IV and β -HAD), indicating increased mitochondrial oxidation. Additionally, in line with our hypothesis, Chadt et al. found that mice lacking TBCID1 (a paralogue of Rab-GTPase activating proteins), TBCID4 or both (TBCID1/TBCID4) had equally increased levels of fatty acid oxidation in the analyzed isolated glycolytic skeletal muscles. Moreover, in contrast with the aforementioned finding the soleus (an oxidative muscle) fatty acid oxidation was elevated only in the mice with TBCID1 knockout and did not change in the case of TBCID1/TBCID4 knockout animals (Chadt et al., 2015). Thus, the authors speculated that β -oxidation in the soleus is more complex process requiring the involvement of other additional factors. Furthermore, these differences might be a result of tissue-specific expression of both proteins, since TBCID1 is expressed predominantly in glycolytic muscles, whereas TBCID4 is mostly present in the oxidative ones (Chadt et al., 2015). Moreover, also other results reported by Maher et al. (2014) confirmed that TBCID1 inhibits fatty acid oxidation by decreasing the activity of β -HAD—a mitochondrial enzyme acting in the β -oxidation pathway. Nevertheless, our present investigation has shed some

light on the role of TBC1D4 with respect to myocellular lipid milieu with some potential implications for myocyte insulin resistant states. Some of the previous research conducted in humans and animal models (Lovejoy et al., 2002; Lee et al., 2006; Lionetti et al., 2014) indicate that the amount of saturated/unsaturated FFA is an important factor when examining the metabolic impact of FA. Generally speaking, the increase of SAT availability promotes diacylglycerol and ceramide accumulation in skeletal muscle cells. However, this enhanced FA esterification into DAG is associated with the pathogenesis of insulin resistance (Schmitz-Peiffer, 2000). Although, there was a significant decrease in DAG fractions accompanied by the reduction in both SAT and MUFA. In this respect, we speculate that AS160 silencing was sufficient to prevent DAG accumulation even with prior prolonged (16 h) incubation with palmitate. Moreover, in our study we found a diminished amount of PL probably caused by decreased amounts of SAT and MUFA, with concomitantly increased n-3 PUFA content. It is quite well recognized that polyunsaturated n-3 fatty acids, for example, eicosapentaenoic or docosahexaenoic acid, are known to prevent or alleviate insulin resistance (Lee et al., 2006). Importantly, phospholipid composition and saturation status influences plasma membrane fluidity and permeability, thus contributing to the membrane protein turnover and proper functioning of its receptors (including insulin receptor) (Hoeks et al., 2011). Therefore, more saturated PL would translate into stiffer plasma membranes, which could potentially influence membrane GLUT-4 transporters availability and/or insulin receptors expression, thus impairing insulin signaling pathway. Therefore, our results indicate that under potentially damaging conditions (palmitate incubation) post-PA-silencing of AS160 significantly decreases the lipotoxic effect of PA contributing to a reduction in DAG and PL content. Importantly, both of the abovementioned lipids are compounds with the potential to promote insulin resistance in myotubes *in vitro*. Remarkably, this is in contrast with the pre-PA-silencing of AS160 group in which AS160 knockdown had virtually no influence on lipid pool(s) or fatty acids composition and most of the observed changes could be attributed to palmitate treatment itself.

Taken altogether, our results reveal that the exposure of L6 skeletal muscle cells to an increased concentration of palmitate with subsequent modest knockdown of AS160 stimulates palmitic acid uptake by promoting an increase in the expression of FAT/CD36, FATP-1, 4. Interestingly, this intervention generally decreases intramyocellular lipid content (DAG, TAG, and PL) due to the increased FA oxidation rate. However, the opposite effect was observed in the group with pre-PA-silencing of AS160 in which we detected elevated expression of FA transporters together with intensified FAs influx, yet without any differences in the lipid pool(s) (AS160⁻/PA vs. PA itself).

Literature Cited

- Blaak EE. 2005. Metabolic fluxes in skeletal muscle in relation to obesity and insulin resistance. *Best Pract Res Clin Endocrinol Metab* 19:391–403.
- Bonen A, Parolin ML, Steinberg GR, Calles-Escandon J, Tandon NN, Glatz JF, Luiken JJ, Heigenhauser GJ, Dyck DJ. 2004. Triacylglycerol accumulation in human obesity and type 2 diabetes is associated with increased rates of skeletal muscle fatty acid transport and increased sarcolemmal FAT/CD36. *Faseb J* 18:1144–1146.
- Bradley H, Shaw CS, Worthington PL, Shepherd SO, Cocks M, Wagenmakers AJ. 2014. Quantitative immunofluorescence microscopy of subcellular GLUT4 distribution in human skeletal muscle: Effects of endurance and sprint interval training. *Physiol Rep* 2: e12085-e12100. <https://www.ncbi.nlm.nih.gov/pubmed/25052490>
- Cameron-Smith D, Burke LM, Angus DJ, Tunstall RJ, Cox GR, Bonen A, Hawley JA, Hargreaves M. 2003. A short-term, high-fat diet up-regulates lipid metabolism and gene expression in human skeletal muscle. *Am J Clin Nutr* 77:313–318.
- Cartee GD. 2015a. Mechanisms for greater insulin-stimulated glucose uptake in normal and insulin-resistant skeletal muscle after acute exercise. *Am J Physiol Endocrinol Metab* 309: E949–E959.
- Cartee GD. 2015b. Roles of TBC1D1 and TBC1D4 in insulin- and exercise-stimulated glucose transport of skeletal muscle. *Diabetologia* 58:19–30.
- Chabowski A, Zdzienicka-Piotrowska M, Miklosz A, Lukaszuk B, Kurek K, Gorski J. 2013. Fiber specific changes in sphingolipid metabolism in skeletal muscles of hyperthyroid rats. *Lipids* 48:697–704.
- Chadt A, Immisch A, de Wendt C, Springer C, Zhou Z, Stermann T, Holman GD, Loffing-Cueni D, Loffing J, Joost HG, Al-Hasani H. 2015. Deletion of both Rab-GTPase-activating proteins TBC1D1 and TBC1D4 in mice eliminates insulin- and AICAR-stimulated glucose transport [corrected]. *Diabetes* 64:746–759.
- Chavez JA, Summers SA. 2003. Characterizing the effects of saturated fatty acids on insulin signaling and ceramide and diacylglycerol accumulation in 3T3-L1 adipocytes and C2C12 myotubes. *Arch Biochem Biophys* 419:101–109.
- Cho NH, Whiting D, Forouhi N, Guariguata L, Hambleton I, Li R, Majeed A, Mbanya JC, Aschner Montoya P, Motala A, Venkat Narayan KM, Ramachandran A, Rathmann W, Roglic G, Shaw J, Silink M, Zhang P. 2015. *IDF Diabetes Atlas*. 7th edition. (ISBN: 978-2-930229-81-2). 9 p.
- Choi K, Kim YB. 2010. Molecular mechanism of insulin resistance in obesity and type 2 diabetes. *Korean J Intern Med* 25:119–129.
- Coburn CT, Knapp FF, Jr., Febbraio M, Beets AL, Silverstein RL, Abumrad NA. 2000. Defective uptake and utilization of long chain fatty acids in muscle and adipose tissues of CD36 knockout mice. *J Biol Chem* 275:32523–32529.
- Coll T, Eyre E, Rodriguez-Calvo R, Palomer X, Sanchez RM, Merlos M, Laguna JC, Vazquez-Carrera M. 2008. Oleate reverses palmitate-induced insulin resistance and inflammation in skeletal muscle cells. *J Biol Chem* 283:11107–11116.
- Constit LA, Bell JA, Houmar J. 2009. Intramuscular lipid metabolism, insulin action, and obesity. *IUBMB Life* 61:47–55.
- Constantinescu S, Turcotte LP. 2013. Genetic downregulation of receptor-interacting protein 140 uncovers the central role of Akt signalling in the regulation of fatty acid oxidation in skeletal muscle cells. *Exp Physiol* 98:514–525.
- DeLany JP, Windhauser MM, Champagne CM, Bray GA. 2000. Differential oxidation of individual dietary fatty acids in humans. *Am J Clin Nutr* 72:905–911.
- Dimopoulos N, Watson M, Sakamoto K, Hundal HS. 2006. Differential effects of palmitate and palmitoleate on insulin action and glucose utilization in rat L6 skeletal muscle cells. *Biochem J* 399:473–481.
- Dyck DJ, Steinberg G, Bonen A. 2001. Insulin increases FA uptake and esterification but reduces lipid utilization in isolated contracting muscle. *Am J Physiol Endocrinol Metab* 281: E600–E607.
- Eckardt K, Taube A, Eckel J. 2011. Obesity-associated insulin resistance in skeletal muscle: Role of lipid accumulation and physical inactivity. *Rev Endocr Metab Disord* 12:163–172.
- Enomoto A, Murakami H, Asai N, Morone N, Watanabe T, Kawai K, Murakumo Y, Usukura J, Kaibuchi K, Takahashi M. 2005. Akt/PKB regulates actin organization and cell motility via Girdin/APE. *Dev Cell* 9:389–402.
- Folch J, Lees M, Sloane Stanley GH. 1957. A simple method for the isolation and purification of total lipides from animal tissues. *J Biol Chem* 226:497–509.
- Frosig C, Richter EA. 2009. Improved insulin sensitivity after exercise: Focus on insulin signaling. *Obesity (Silver Spring)* 17:S15–S20.
- Gao D, Griffiths HR, Bailey CJ. 2009. Oleate protects against palmitate-induced insulin resistance in L6 myotubes. *Br J Nutr* 102:1557–1563.
- Gaster M, Rustan AC, Beck-Nielsen H. 2005. Differential utilization of saturated palmitate and unsaturated oleate: Evidence from cultured myotubes. *Diabetes* 54:648–656.
- Hargrett SR, Walker NN, Keller SR. 2015. Rab GAPs AS160 and Tbc1d1 play non-redundant roles in the regulation of glucose and energy homeostasis in mice. *Am J Physiol Endocrinol Metab* 310:E276–E288. <https://www.ncbi.nlm.nih.gov/pubmed/26625902>
- Hegarty BD, Cooney GJ, Kraegen EW, Furler SM. 2002. Increased efficiency of fatty acid uptake contributes to lipid accumulation in skeletal muscle of high fat-fed insulin-resistant rats. *Diabetes* 51:1477–1484.
- Hoeks J, Wilde J, Hulshof MF, Berg SA, Schaart G, Dijk KW, Smit E, Mariman EC. 2011. High fat diet-induced changes in mouse muscle mitochondrial phospholipids do not impair mitochondrial respiration despite insulin resistance. *PLoS ONE* 6:e27274.
- Karlsson HK, Zierath JR, Kane S, Krook A, Lienhard GE, Wallberg-Henriksson H. 2005. Insulin-stimulated phosphorylation of the Akt substrate AS160 is impaired in skeletal muscle of type 2 diabetic subjects. *Diabetes* 54:1692–1697.
- Knapp P, Chabowski A, Posmyk R, Gorski J. 2016. Expression of the energy substrate transporters in uterine fibroids. *Prostaglandins Other Lipid Mediat* 123:9–15.
- Lansley MN, Walker NN, Hargrett SR, Stevens JR, Keller SR. 2012. Deletion of Rab GAP AS160 modifies glucose uptake and GLUT4 translocation in primary skeletal muscles and adipocytes and impairs glucose homeostasis. *Am J Physiol Endocrinol Metab* 303: E1273–E1286.
- Lee JS, Pinnamaneni SK, Eo SJ, Cho IH, Pyo JH, Kim CK, Sinclair AJ, Febbraio MA, Watt MJ. 2006. Saturated, but not n-6 polyunsaturated, fatty acids induce insulin resistance: Role of intramuscular accumulation of lipid metabolites. *J Appl Physiol* (1985) 100:1467–1474.
- Lionetti L, Mollica MP, Sica R, Donizetti I, Gifuni G, Pignatola A, Cavaliere G, Putti R. 2014. Differential effects of high-fish oil and high-lard diets on cells and cytokines involved in the inflammatory process in rat insulin-sensitive tissues. *Int J Mol Sci* 15:3040–3063.
- Lovejoy JC, Most MM, Lefevre M, Greenway FL, Rood JC. 2002. Effect of diets enriched in almonds on insulin action and serum lipids in adults with normal glucose tolerance or type 2 diabetes. *Am J Clin Nutr* 76:1000–1006.
- Lukaszuk B, Miklosz A, Chabowski A, Gorski J. 2015. Modest decrease in PGC1alpha results in TAG accumulation but not in insulin resistance in L6 myotubes. *Cell Physiol Biochem* 35:1609–1622.
- Maher AC, McFarlan J, Lally J, Snook LA, Bonen A. 2014. TBC1D1 reduces palmitate oxidation by inhibiting beta-HAD activity in skeletal muscle. *Am J Physiol Regul Integr Comp Physiol* 307:R1115–R1123.
- Manrique C, Sowers JR. 2014. Insulin resistance and skeletal muscle vasculature: Significance, assessment and therapeutic modulators. *Cardiovasc Med* 4:244–256.
- Martins AR, Nachbar RT, Gorjao R, Vinolo MA, Festecca WT, Lambertucci RH, Cury-Boaventura MF, Silveira LR, Curi R, Hirabara SM. 2012. Mechanisms underlying skeletal muscle insulin resistance induced by fatty acids: Importance of the mitochondrial function. *Lipids Health Dis* 11:30.
- Miklosz A, Lukaszuk B, Zdzienicka-Piotrowska M, Kurek K, Chabowski A. 2016. The effects of AS160 modulation on fatty acid transporters expression and lipid profile in L6 myotubes. *Cell Physiol Biochem* 38:267–282.
- Mukherjee B, Hossain CM, Mondal L, Paul P, Ghosh MK. 2013. Obesity and insulin resistance: An abridged molecular correlation. *Lipid Insights* 6:1–11.
- Nickerson JG, Alkhatieb H, Benton CR, Lally J, Nickerson J, Han XX, Wilson MH, Jain SS, Snook LA, Glatz JF, Chabowski A, Luiken JJ, Bonen A. 2009. Greater transport efficiencies of the membrane fatty acid transporters FAT/CD36 and FATP4 compared with FABPpm and FATP1 and differential effects on fatty acid esterification and oxidation in rat skeletal muscle. *J Biol Chem* 284:16522–16530. <https://www.ncbi.nlm.nih.gov/pubmed/19380575>
- Ouwens DM, Diamant M, Fodor M, Habets DD, Pelsers MM, El Hasnaoui M, Dang ZC, van den Brom CE, Vlasblom R, Rietdijk A, Boer C, Coort SL, Glatz JF, Luiken JJ. 2007.

- Cardiac contractile dysfunction in insulin-resistant rats fed a high-fat diet is associated with elevated CD36-mediated fatty acid uptake and esterification. *Diabetologia* 50:1938–1948.
- Roberts PJ, Der CJ. 2007. Targeting the Raf-MEK-ERK mitogen-activated protein kinase cascade for the treatment of cancer. *Oncogene* 26:3291–3310.
- Sakamoto K, Holman GD. 2008. Emerging role for AS160/TBC1D4 and TBC1D1 in the regulation of GLUT4 traffic. *Am J Physiol Endocrinol Metab* 295:E29–E37.
- Samovski D, Su X, Xu Y, Abumrad NA, Stahl PD. 2012. Insulin and AMPK regulate FA translocase/CD36 plasma membrane recruitment in cardiomyocytes via Rab GAP AS160 and Rab8a Rab GTPase. *J Lipid Res* 53:709–717.
- Samuel VT, Petersen KF, Shulman GI. 2010. Lipid-induced insulin resistance: Unravelling the mechanism. *Lancet* 375:2267–2277.
- Sano H, Kane S, Sano E, Miinea CP, Asara JM, Lane WS, Garner CW, Lienhard GE. 2003. Insulin-stimulated phosphorylation of a Rab GTPase-activating protein regulates GLUT4 translocation. *J Biol Chem* 278:14599–14602.
- Schimanski S, Wild PJ, Trecek O, Horn F, Sigrüener A, Rudolph C, Blaszyk H, Klinkhammer-Schalke M, Ortmann O, Hartmann A, Schmitz G. 2010. Expression of the lipid transporters ABCA3 and ABCA1 is diminished in human breast cancer tissue. *Horm Metab Res* 42:102–109.
- Schmitz-Peiffer C. 2000. Signalling aspects of insulin resistance in skeletal muscle: Mechanisms induced by lipid oversupply. *Cell Signal* 12:583–594.
- Schwenk RW, Holloway GP, Luiken JJ, Bonen A, Glatz JF. 2010. Fatty acid transport across the cell membrane: Regulation by fatty acid transporters. *Prostaglandins Leukot Essent Fatty Acids* 82:149–154.
- Seyoum B, Fite A, Abou-Samra AB. 2011. Effects of 3T3 adipocytes on interleukin-6 expression and insulin signaling in L6 skeletal muscle cells. *Biochem Biophys Res Commun* 410:13–18.
- Szekeress F, Chadt A, Tom RZ, Deshmukh AS, Chibalin AV, Bjornholm M, Al-Hasani H, Zierath JR. 2012. The Rab-GTPase-activating protein TBC1D1 regulates skeletal muscle glucose metabolism. *Am J Physiol Endocrinol Metab* 303:E524–E533.
- van der Vusse GJ, Roemen TH, Reneman RS. 1980. Assessment of fatty acids in dog left ventricular myocardium. *Biochim Biophys Acta* 617:347–349.
- Vind BF, Pehmoller C, Treebak JT, Birk JB, Hey-Mogensen M, Beck-Nielsen H, Zierath JR, Wojtaszewski JF, Hojlund K. 2011. Impaired insulin-induced site-specific phosphorylation of TBC1 domain family, member 4 (TBC1D4) in skeletal muscle of type 2 diabetes patients is restored by endurance exercise-training. *Diabetologia* 54:157–167.
- Wong MH, Xue A, Baxter RC, Pavlakis N, Smith RC. 2016. Upstream and downstream co-inhibition of mitogen-activated protein kinase and PI3K/Akt/mTOR pathways in pancreatic ductal adenocarcinoma. *Neoplasia* 18:425–435.
- Yuzefovych L, Wilson G, Racheck L. 2010. Different effects of oleate vs. palmitate on mitochondrial function, apoptosis, and insulin signaling in L6 skeletal muscle cells: Role of oxidative stress. *Am J Physiol Endocrinol Metab* 299:E1096–E1105.